A Study on the Paul-Baker System as an Instrument for Multi-object Spectrum Observation

Xiang-Yan Yuan[1], Ding-Qiang Su[1,2], Xiang-Qun Cui[1] and Gen-Rong Liu[1]

[1] National Astronomical Observatories, Nanjing Institute of Astronomical Optics &
    Technology, Chinese Academy of Sciences, Nanjing 210042; *xyyuan@niaot.ac.cn*
[2] Department of Astronomy, Nanjing University, Nanjing 210093

Abstract Paul-Baker systems with 4° flat field and 5° flat field are studied. Their light obstructions under different f/ratios of the primary mirror are analyzed. Due to the strong f/ratio of the system, a focal length extender is designed in order to match the following fiber instrumentation, and two kinds of dispersion prism correctors are designed for correcting the atmospheric dispersion. We compare the designed Paul-Baker system with LAMOST, the national major scientific project now under construction.

Key words: techniques: telescopes — instrumentation: miscellaneous

1 INTRODUCTION

Astronomical optics is trending towards telescopes with large aperture, faster f/ratio and using more aspheric surfaces. Astronomical telescopes used for multi-object spectrum observations also require a wide field of view (FOV). The three-mirror system, typified by the Paul-Baker system and the Willstrop system, has been fully researched because of its compact configuration and good image quality over a wide FOV. The large sky area multi-object fiber spectroscopic telescope (LAMOST) is a system intended for multi-object spectrum observations; it is a unique reflecting Schmidt telescope with both a large aperture and a wide FOV. Before the LAMOST scheme was decided on, the Paul-Baker system was considered too, but was discarded due to the heavy obstruction and high price. This paper first studies the Paul-Baker system, then calculates the light obstructions for a 4° diameter field and a 5° diameter field under different f/ratios of the primary mirror. A comparison with LAMOST is given at the end.

2 LIGHT OBSTRUCTION IN PAUL-BAKE SYSTEM WITH 4° AND 5° FIELD OF VIEW

The first well-corrected telescope system using three curved mirrors, as shown in Figure 1, was proposed by Paul (1935), which includes a paraboloidal primary mirror M1, a spherical convex
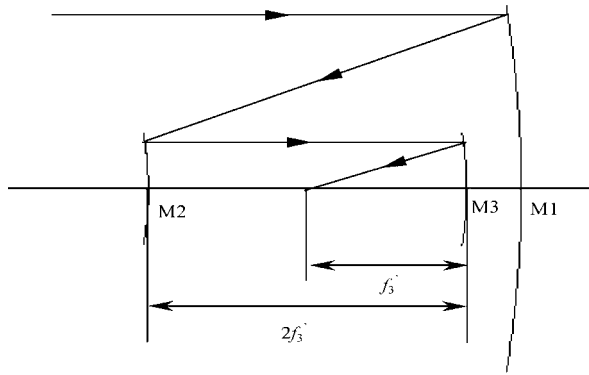
Fig. 1 A three mirror system suggested by Paul (Wilson 1996).

secondary mirror M2 and a spherical tertiary mirror M3. The original Paul form starts off with a parallel beam compressor composed of two confocal paraboloids (Wilson 1996). Paul added a spherical tertiary mirror to the beam compressor, placing it so that its center of curvature is at the vertex of the secondary. This tertiary introduces spherical aberration, but also functions as a Schmidt primary receiving a beam from the exit pupil of the beam compressor, if the exit pupil is placed at the secondary. Paul corrected the spherical aberration in an elegant way by letting $r3 = r2$ ($r2$ and $r3$ are the radius of curvature of M2 and M3, respectively) and added an aspheric surface on the secondary mirror to make it also spherical. It can be proved that such a system is free of spherical aberration, coma and astigmatism at the same time, but the field is not flat, and has a curvature radius the same as the primary mirror. However, as a matter of fact, any three mirror system can eliminate spherical aberration, coma and astigmatism at the same time; this is demonstrated in Su (1984) in detail.

Baker modified Paul's system by making $|r3| > |r2|$ and changing the secondary to ellipsoidal, then the Petzval sum is zero and a flat field is achieved (Baker 1969). Since then such a system is known as the Paul-Baker system. The Willstrop system is also of the same type (Willstrop 1984), being composed of a parabolic primary, a spherical secondary and a spherical tertiary mirror, but the tertiary is placed far behind the primary, and the curved focal surface is at the plane of the primary. The Willstrop telescope with 5 m aperture and 4° diameter field can obtain good quality images with rms image spot diameter of 0.263 arcsecond. However, the diameters of the secondary and the tertiary mirror are 2.643m and 3.53 m, respectively, the price for such a system is very high, and the obstruction due to the primary perforation is large, so the energy loss is quite heavy.

This paper will examine the Paul-Baker system with a 4° diameter field and a 5° diameter field, analyze the relationship between light obstruction and image quality, and discuss the possibility using the Paul-Baker system for astronomical spectrum survey.

2.1 Calculations and Analysis

The optical configuration of large field Paul-Baker system is shown in Figure 2. L1 and L2 represent respectively the distance from the primary focus to the vertices of the primary and the secondary.

The surface shapes of the primary, secondary and the tertiary mirrors are all symmetrically rotating high order aspheric. The surface sag can be expressed as

$$x = \frac{cy^2}{1 + \sqrt{1 - c^2(1+k)y^2}} + A_3 y^6 + A_4 y^8 + A_5 y^{10}, \tag{1}$$
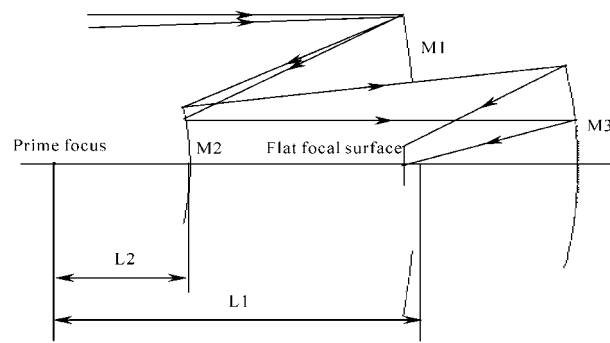
Fig. 2 Scheme of Paul-Baker system with flat field.

where c denotes the vertex curvature of the aspherical surface and k is the conic coefficient. A_3, A_4, and A_5 are the coefficients of high order aspheric. Optimization variables in system design are $k1$, $k2$, $k3$, A_{13}, A_{14}, A_{15}, A_{23}, A_{24}, A_{25}, A_{33}, A_{34}, A_{35}, $r3$ and $d2$ ($d3=r3/2$); $r3$ is the curvature radius of the tertiary mirror, $d2$ the distance from the secondary mirror to the tertiary mirror and $d3$ the distance from the tertiary mirror to the focal surface.

The light obstruction of Paul-Baker system consists of two parts. The first is caused by the primary perforation. The corresponding light obstruction ratio in diameter can be expressed as $b1 = D_0/D_1$, here D_0 is the diameter of perforation on primary mirror, and D_1 is the diameter of primary mirror; the second is the focal surface obstruction which is given by $b2 = D_4/D_2$, here D_4 is the diameter of the focal surface and D_2 is the diameter of the axial beam of the secondary mirror ($2h_2$). In Tables 1 and 2 are listed the calculation results of the light obstruction ratio in diameter, $b1$ and $b2$, the corresponding image spot diameter for the Paul-Baker system with $4°$ and $5°$ of FOV respectively, and under different primary f/ratios. All the results obtained are independent of the system aperture. The system parameters can be scaled according to the design requirement.

The image performance of the designed system at the maximum FOV is given not only by the RMS (root-mean-square) image spot, but also by the geometrical image spot diameter, both of which diameter, but also by Geo (Geometrical) image spot diameter, are represented by a corresponding angle in the sky in units of arcsecond. The last column in the two tables lists the system f/ratio which is optimized but without other restrictions.

From the two tables we can see: (1) The light obstruction on primary mirror $b1$ is always larger than $b2$, so the light obstruction of the Paul-Baker system is $b1$, which is larger than 50%. In addition, the light directly reaching the tertiary through the perforation of the primary mirror will generate stray light, so baffles should be arranged between the primary and the secondary, which will increase the light obstruction. (2) The minimum of $b1$ is included in the secondary position defined by L_2/L_1 from 0.28 to 0.43. Moving the secondary M2 towards the primary focus can make the diameter of M2 smaller, which can lower the light obstruction $b1$, increase the light obstruction on the secondary $b2$, and worsen the image quality. However, there is a best position for moving, further moving M2 will increase the light obstruction on primary mirror due to the spread of the light beam, and deteriorate the image quality, which can be seen in the tables when the secondary position (L_2/L_1) changes from 1/3 to 0.28. (3) For a fixed primary f/ratio, if different positions of the secondary give almost the same obstruction but varying image quality, then the position of secondary should be determined by the image quality. (4) For the Paul-Baker system with $4°$ FOV, when the primary f/ratio is 1, the minimum obstruction is 52.2%; when f/ratio is 1.2, the minimum obstruction is 56%; and

Table 1   Calculated results of the light obstruction ratio in diameter and the image spot diameter for Paul-Baker system of 4° FOV with different primary f/ratio

Primary f/ratio	Secondary Position L_2/L_1	Light Obstruction		Image Spot Diameter		System f/ratio
		$b1$	$b2$	Rms	Geo	
1	0.28	0.524	0.360	1.638	3.466	1.434
	0.30	0.522	0.344	1.361	2.925	1.471
	1/3	0.527	0.324	1.031	2.212	1.540
	0.40	0.551	0.297	0.619	1.368	1.701
1.2	0.28	0.565	0.429	1.073	2.062	1.709
	0.30	0.560	0.411	0.928	1.880	1.754
	1/3	0.562	0.386	0.701	1.423	1.836
	0.40	0.579	0.356	0.416	0.812	2.031
1.5	0.28	0.631	0.533	0.660	1.125	2.124
	0.30	0.621	0.511	0.557	0.969	2.181
	1/3	0.615	0.481	0.413	0.734	2.284
	0.40	0.621	0.443	0.248	0.447	2.528

Table 2   Calculated results of the light obstruction ratio in diameter and the image spot diameter for Paul-Baker system of 5° FOV with different primary f/ratios

Primary f/ratio	Secondary Position L_2/L_1	Light Obstruction		Image Spot Diameter		System f/ratio
		$b1$	$b2$	Rms	Geo	
1	0.28	0.581	0.454	3.094	6.062	1.441
	0.30	0.573	0.434	2.60	5.177	1.478
	1/3	0.573	0.407	1.960	4.009	1.545
	0.40	0.587	0.374	1.155	2.242	1.705
1.2	0.28	0.635	0.541	2.042	3.485	1.717
	0.30	0.622	0.517	1.712	2.983	1.761
	1/3	0.616	0.486	1.320	2.378	1.843
	0.40	0.622	0.446	0.786	1.423	2.036
1.5	0.30	0.698	0.642	1.073	1.642	2.188
	1/3	0.684	0.603	0.949	1.753	2.284
	0.40	0.675	0.556	0.474	0.793	2.534
	0.43	0.677	0.543	0.392	0.663	2.663

for a primary f/ratio 1.5 the minimum obstruction increases to 61.5%. For the 5° FOV Paul-Baker system, the corresponding minimum light obstructions are 57.3%, 61.6% and 67.5%. This means the bigger the primary f/ratio is, the better the image quality, but the larger the light obstruction is as well. So, if there is no very high image quality demanded and no problem with the necessary mirror manufacturing technique, then a strong primary f/ratio can be selected. In other words, when determining the primary f/ratio both the obstruction and the image quality should be taken into consideration.
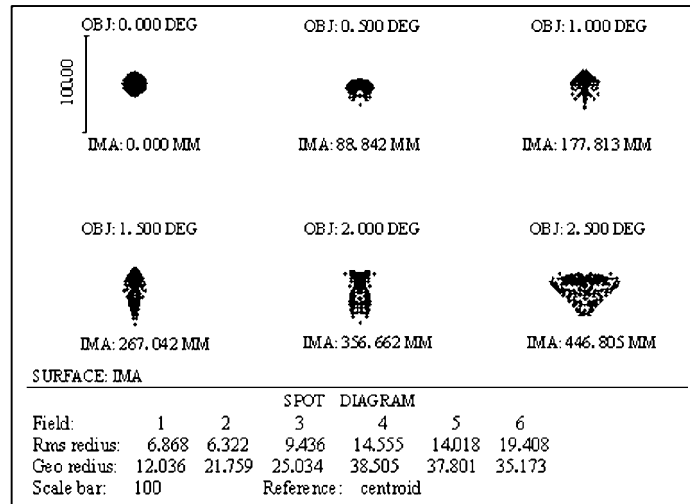
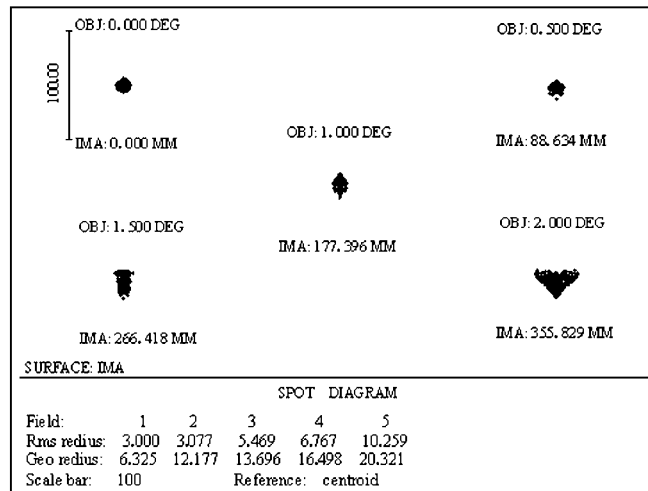**Fig. 3** Image spot diagram for the system of 5° FOV.

Fig. 4 Image spot diagram for the system of 4o FOV.

2.2 Design Examples

As an example, a system with 5 m aperture, 5° FOV, primary f/ratio 1.2 and L2/L1=0.40 is designed. The designing data are listed in Table 3 and the image spot diagram is shown by Figure 3. Table 4 and Figure 4 show the parameters and the image spot diagram of another system, with 5m aperture, 4° FOV, primary f/ratio 1.2 and L2/L1=0.40, optimized with the same variables.

The optimized 5° FOV system has a flat field with system f/ratio 2.036, of which the RMS image spot diameter is 0.786″ at the maximum FOV position, and the light obstruction ratio

Table 3 Designed system with aperture 5 m, FOV 5° in diameter and primary f/ratio 1.2

Surface number	1 (stop)	2	3	4
Surface type	Even aspheric	Even aspheric	Even aspheric	Image plane
Vertex radius of curvature (mm)	−12000	−4800	−8142.648	infinity
Separation (mm)	−3600	7631.435	−4071.335	
Glass	Mirror	Mirror	Mirror	
Semi-diameter (mm)	2511.471	1157.756	1991.853	446.804
Conic coefficient	−1.0319	−0.8763	−0.0114	
A3	-1.6180×10^{-23}	-1.7440×10^{-20}	-1.5603×10^{-21}	
A4	-2.5095×10^{-30}	-5.8616×10^{-27}	1.9719×10^{-28}	
A5	1.7031×10^{-37}	2.0282×10^{-33}	-1.4776×10^{-35}	

Table 4 Designed system with aperture 5 m, FOV 4° in diameter and primary f/ratio 1.2

Surface number	1 (stop)	2	3	4
Surface type	Even aspheric	Even aspheric	Even aspheric	Image plane
Vertex radius of curvature (mm)	−12000	−4800	−8123.481	infinity
Separation (mm)	−3600	7646.702	−4061.739	
Glass	Mirror	Mirror	Mirror	
Semi-diameter (mm)	2509.158	1126.594	1802.464	355.832
Conic coefficient	−1.0286	−0.8661	−0.0056	
A3	-1.9516×10^{-23}	-1.9592×10^{-20}	-1.2178×10^{-21}	
A4	-2.2507×10^{-30}	-4.4216×10^{-27}	1.1670×10^{-28}	
A5	1.3925×10^{-37}	1.4412×10^{-33}	-7.0806×10^{-36}	

in diameter is 62.2%. For the 4° FOV system, the system f/ratio is 2.031 and the maximum RMS image spot diameter is 0.416″, the light obstruction ratio in diameter is 57.9%.

3 DESIGN OF THE FOCAL LENGTH EXTENDER

In order to match the f/ratio of fiber, f/ratio conversion should be made for the fast f/ratio Paul-Baker system. As is well known, there are three pairs of conjugated points for a single refracting surface. The one determined by the following formula is free from spherical aberration and satisfies the sine condition (Lin 1960),

$$l = \frac{n + n'}{n} r \, , \qquad l' = \frac{n + n'}{n'} r.$$

Here n and n' are the object space (glass material) refractive index and the image space (air) refractive index respectively; r is the curvature radius of the refractive surface. Let the first surface be concentric with the system focus, and the second surface be calculated according to the above formula. The two new added surfaces will not introduce new spherical aberration or coma, but will introduce chromatic aberration. So we add a cemented surface between the two, the material used in such a cemented lens is F2 and ZK11. In order to keep the system's focal

length fixed, $r2$ should be changed. The new $r2'$ and $r2$ satisfy the following relation,

$$\frac{r2'}{r2} = \frac{n2 - 1}{n1 - 1}.$$

Figure 5 shows one of the designed achromatic focal length extender, with $r1 = -11\,\text{mm}$, $r2 = 340.2\,\text{mm}$, and $r3 = -5.76\,\text{mm}$. Putting the extender at $11\,\text{mm}$ before the system's focus will make the f/ratio $n1$ times the original f/ratio.

The f/ratio can also be changed with a part conic optical fiber (Su et al. 1986). The transmission of light in the fiber also satisfies the Lagrange Invariant. So, selecting a part of conic fiber with smaller entrance diameter and larger exit diameter can realize the f/ratio conversion. This method is simple in structure, and introduces no chromatic aberration. Also, techniques are available to couple such a conic optical fiber with following fiber equipments.

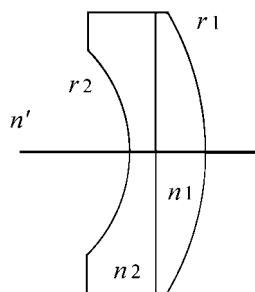## 4 DESIGN OF THE ATMOSPHERIC DISPERSION PRISM

Atmospheric refraction varies with wavelength and the light with a different wavelength will follow a different curve when passing through the atmosphere layer. This is the cause of atmospheric dispersion which makes the star image change from a point to a spectrum, and the energy dispersion blurs the originally clear image. Thus, it should be corrected.

There are two methods to make the correction. The first is by adding prisms or lensms (lens-prisms) before the focal plane (Su 1986), or by adding correctors and prism before the focal plane such as in the GSMT wide field system (Strom & Stepp 2002) and the LSST (see http://www.lsst.org/Project/docs/SPIE_4836-19_10-01-02.pdf), to correct the dispersion over the whole field, but such a correcting system is very expensive. The second is the one adopted here, i.e., by adding a small dispersion corrector before each fiber to have the atmospheric dispersion of each star image corrected before entering the fiber (Su et al. 1986). The small correctors are near the focal plane, so the image quality is good and the price is lower. However, this method will introduce a problem of parallactic angle when the celestial object is away from the meridian (Liu & Yuan 2005).

The atmosphere will generate a dispersion about $5''$ at about zenith $70°$. Accordingly, the designed dispersion correcting prism should produce a reverse dispersion of $5''$. Here we also adopt the method of concentric prism designed by Liu (Liu & Yuan 2005). Because of the Paul-Baker system's strong f/ratio and the nearer distance between the dispersion corrector and the focal plane, using only one group of dispersion prisms will require a large tilt angle of the cemented surface, which is quite difficult to realize. In order to correct the atmospheric dispersion of different zenith effectively, and guarantee the tilt angle to be small and the image quality at the center wavelength not deteriorated, we designed two groups of prisms which can rotate around the optical axis. Two cemented surfaces of each group can realize a dispersion of $2.5''$.

In order to obtain a compact configuration of the whole system and easy adjustment, we integrate the designed focal length extender and the atmospheric dispersion corrector by making the last surface of the dispersion prism and the first surface of the focal length extender into one, as shown in Figure 6. The parameters of the surfaces including the curvature radius, thickness, tilted angle, and selected glass material, are listed in Table 5. The sequence of surfaces is from right to left (the input light comes from the right).

We put the designed dispersion corrector and focal length extender into a perfect optical system with focal length $7345.12\,\text{mm}$ and f/ratio 1.836 (which corresponds to the Paul-Baker system listed in Table 1, with primary f/ratio 1.2 and $L_2/L_1 = 1/3$), and set the FOV to zero. The image spot diameters and dispersion value generated by one group of atmospheric dispersion correctors (surfaces from 1 to 6 in Table 5) are listed in Table 6. Table 7 lists the results of

Fig. 5 Diagram of the achromatic focal length extender.
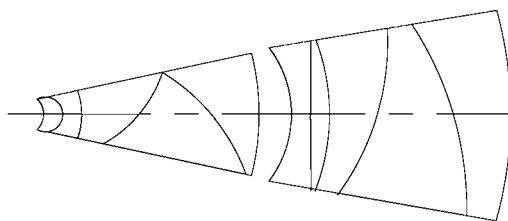
Fig. 6 Diagram of atmospheric dispersion corrector and focal length extender.
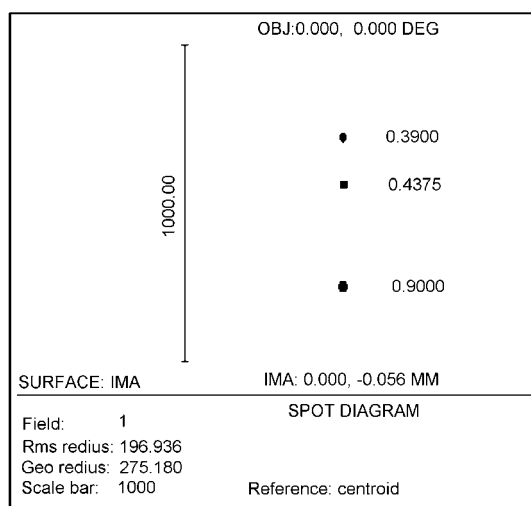
Table 5 Parameters of Atmospheric Dispersion Corrector and Focal Length Extender

Surface Number	Radius of curvature (mm)	Thickness (mm)	Clear aperture (mm)	Tilted angle (°)	Glass
1	20.5	-3	11.13	0	QF1
2	−17.5	−4	10.25	−16.3	BAK4
3	−13.5	−2.5	7.91	16.3	QF1
4	−11	−1	5.99	0	F2
5	340.21	−1	5.67	0	ZK11
6	−5.76	−1.72	4.83	0	air
7	−13	−2.5	4.38	0	QF1
8	−10.5	−3.8	4.82	40	BAK4
9	−6.7	-3	3.08	40	QF1
10	−3.7	−1	1.41	0	ZK11
11	−0.88	−1	1.05	0	F2
12	−1.11	−2.81	0.78	0	

the two groups of atmospheric dispersion correctors described in Table 5. Figure 7 presents the corresponding spot diagram. The adopted working wavelength band is 0.39–0.9 μm, and the center wavelength is 0.4375 μm.

From Tables 6, 7 and Figure 7, we can see by inserting two groups of the atmospheric dispersion corrector and focal length extender designed in this paper into the Paul-Baker system and making it rotate around the optical axis to realize the sum and subtraction of two dispersions generated by each of the group, the different atmospheric dispersions of different observing sky areas can be corrected effectively. Another advantage is the easy connection with the following fiber arrangement.

As for the 5″ dispersion, the residual dispersion caused by the parallactic angle after correcting will exceed 1″, which can not be neglected. So, a special structure with good torsion stiffness must be designed to guarantee small correctors to point to the zenith all the time. For example, placing the small corrector at the head of the fiber, and a ball bearing is set on the fiber head to make the fiber free from rotation. This method can solve the problem of paral-

Fig. 7 Spot diagram generated by two groups of atmospheric dispersion corrector and focal length extender.

Table 6 Image spot diameters and dispersion value generated by one group of atmospheric dispersion corrector and the focal length extender (f'=11989.3, f/ratio=3.108)

Wavelength (μm)	Image spot diameter ($''$)		Image height (mm)	Dispersion value ($''$)
	Rms	Geo		
0.39	0.1	0.124	0.047	
0.4375	0.0582	0.101	0	2.512
0.9	0.0896	0.132	−0.099	

Table 7 Image spot diameters and dispersion value generated by two groups of atmospheric dispersion corrector and the focal length extender ($f' = 19454.2$, f/ratio=5.139)

Wavelength (μm)	Image spot diameter ($''$)		Image height (mm)	Dispersion value ($''$)
	Rms	Geo		
0.39	0.149	0.212	0.152	
0.4375	0.074	0.128	0	5.00
0.9	0.126	0.285	−0.320	

lactic angle, but such a structure is difficult to realize. In practice, some of the sky area can be sacrificed and we only observe areas within 50° of the zenith. So the atmospheric dispersion will be about 2.2$''$, and the dispersions between 1$''$ ∼2.2$''$ can be corrected by the 1.6$''$ correcting prism designed by Liu & Yuan (2005), dispersions less than 1$''$ will not be corrected. This will significantly simplify the correction.
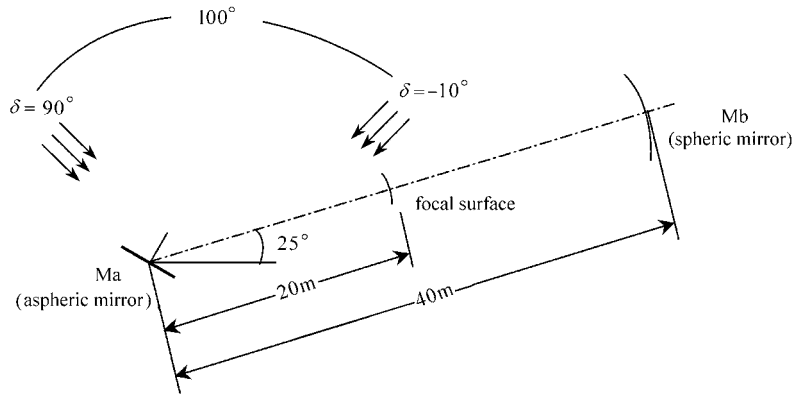
Fig. 8 Optics configuration of LAMOST.

5 COMPARISON OF PAUL-BAKER SYSTEM WITH LAMOST SCHEME

The Paul-Baker system has the following advantages: compact configuration, flat field and better image quality. However, the configuration of this system is composed of three aspherical mirrors of large aperture, so the cost is much higher, and the light obstruction is quite heavy. The stray sky light reflected by the tertiary mirror should be baffled in actual practice and such baffles will further increase the light obstruction. Another disadvantage of the Paul-Baker system is that f/ratio conversion is needed for the match with multi-object optical fiber spectrum instruments because of its strong f/ratio.

LAMOST is a reflecting Schmidt telescope with its main optical axis on the meridian plane tilted at an angle of 25° to the horizontal (Su et al. 1998; Su et al. 2004; Wang et al. 1996). Its configuration diagram is shown in Figure 8. The whole system includes three parts: reflecting Schmidt corrector Ma at the northern end; spherical mirror Mb with curvature radius 40 m at the southern end, which is fixed on the foundation; and focal plane with a linear diameter of 1.75 m in between, which provides the foundation for placing 4000 or more optical fibers on the focal surface, also fixed on its ground bases. This configuration presents a new design mode and leaves out the long tube of traditional Schmidt telescope. An alt-azimuth mounting is adopted for Ma to execute the tracking, and active optics is used for Ma to eliminate the third-order spherical aberration of Mb. The light coming from the celestial objects is first reflected from Ma to Mb, and then reflected by Mb and forms image on the focal plane, where 4000 optical fibers are accurately positioned to feed the light of individual objects into the slits of 16 spectrographs fixed in the room underneath. Then the spectra of the 4000 objects are recorded by a high resolution CCD system simultaneously. Combined with the modern multi-object optical fibers and computer technology, LAMOST will have a large scale sky survey capability.

LAMOST has a clear aperture of 4m and the system f/ratio is 5. Such a f/ratio is suitable for coupling with optical fibers. Ma is composed of 24 hexagonal planar sub-mirrors and Mb consists of 37 hexagonal spherical sub-mirrors. Using segments to replace the whole reflecting mirror greatly reduces the cost and makes a better mirror seeing, smaller gravity deflection, lighter support structure and easier manufacture and transportation. The light obstruction ratio in diameter of LAMOST is only 30.6% caused by the focal surface, which is much smaller than that of the Paul-Baker system.

However, compared to the Paul-Baker system, one shortcoming of LAMOST is that the optimal focal surface is not flat, but an asymmetric curved surface which changes with different

declination and time during one observation. In practice, a spherical surface with a slightly tilted optical axis and a radius of curvature almost the same as that the system's focal length is used as an approximate focal surface. The image quality of LAMOST is not so good as that of the Paul-Baker system due to the special configuration which leads to an image quality that varies with the area and time of observation. Without consideration of the effect of atmospheric refraction, for a one-and-half hours tracking before and after the celestial objects passing through the meridian, the maximum image spread is $1.91''$ at the approximate focal surface (corresponding to declination of $90°$), which can fully satisfy the requirement for image quality in fact.

Ten years ago, when discussing the LAMOST scheme, Xing roposed a parallel controllable optical fiber positioning system, which divides the convex focal plate of the telescope into 4000 little domains, each containing a controllable unit on which an optical fiber is mounted (Xing et al. 1997). This method can reposition the 4000 optical fibers in only several minutes, and compensate many kinds of errors caused by temperature and other factors during observation. However, If such a fiber positioning system is used in the Paul-Baker system, i.e., to mount 4000 optical fibers on the focal plane greatly smaller than that of the LAMOST, the arrangement of the fibers and the positioning system will be very difficult. The Anglo-Australian Observatory has developed a fiber positioning system (Echidna), which has 400 fibers feeding two near infrared spectrographs from the primary focus of the Subaru telescope (Gillingham et al. 2002). Echidna is a piezoelectric actuator driven fiber positioner which can get around the denseness problem of fiber positioning on the focal plane. However, the in-between focal plane will make the operation and adjustment inconvenient. In addition, to manufacture a 5 meter diameter primary mirror with f/ratio 1 or 1.2 was almost impossible ten years ago. It is not easy even now and too expensive. These are the reasons why we did not select the Paul-Baker system.

In conclusion, at the time, it was proper to select LAMOST for a wide field spectroscopic survey instrument; and is even so today; however, today, the Paul-Baker system can also be considered as a proper choice.

References

Baker J. G., 1969, IEEE Trans. Aerosp. Electron. Syst., 5, 261
Gillingham P., Moore A., Akiyama M. et al., 2002, In: M. Lye, A. F. M. Moorwood eds., Proc. SPIE 4841, Instrument Design and Performance for Optical/Infrared Ground-based Telescopes, Part Two, Bellingham: SPIE, p.985
Lin Y. B., 1960, Optical Design Instruction, 36
Liu G. R., Yuan X. Y., 2005, Acta Astronomica Sinica, 46, 3
Paul M., 1935, Rev. d'Opt., 14, 169
Strom S., Stepp L., Gregory B. et al., GSMT Point Design, 2002
Su D. Q., 1984, Optical Instrument Techniques, 2, 20
Su D. Q., 1986, A&A, 156, 381
Su D. Q., Cao C. X., Liang M., 1986, In: L. D. Barr ed., Proc. SPIE 628, Conference on Advanced Technology Optical Telescopes III, 498 Strom
Su D. Q., Cui X. Q., 2004, ChJAA, 4(1), 1
Su D. Q., Cui X. Q., Wang Y. N., Yao Z. Q., 1998, In: L. M. Stepp ed., Proc. SPIE 3352, Conference on Advanced Technology Optical/IR Telescopes VI, 78
Wang S. G., Su D. Q., Chu Y. Q., Cui X. Q., Wang Y. N., 1996, Appl. Opt., 35, 5155
Willstrop R. V., 1984, Mon. Not. R. astr. Soc., 210, 597
Wilson R. N., 1996,Reflecting Telescope Optics 1
Xing X. Z., Hu H. Z., Du H. S. et al., 1997, Transaction of USTC, 4, 27